Normal moveout with phase equalization

Tiago Barros (FEEC/UNICAMP), Marcos Covre (FEEC/UNICAMP), André K. Takahata (DSPGeo) and Renato Lopes (FEEC/UNICAMP)

This paper was prepared for presentation at the 14th International Congress of the Brazilian Geophysical Society, held in Rio de Janeiro, Brazil, August 3-6, 2015.

Abstract

Seismic signals may present large deviations in phase, especially in the case of post-critical reflections. In this paper we propose a method for normal moveout with phase equalization. This method employs the first eigenimage obtained with the use of the singular value decomposition of the analytical signal of seismic windowed data. We present tests of this method in two synthetic data, both of them with post-critical reflections. The initial results indicate that the phase change can be corrected using complex signals. These results must be further confirmed by simulations on real data.

Introduction

Stacking of seismic signals is one operation of great interest in seismic signal processing (Yilmaz, 2001). The main goal of this operation is to generate a simulated zero-offset (ZO) trace. For this trace, the offset between source and receiver is zero, i.e., they are both *virtually* at the same position. The stacked ZO trace has some interesting properties (Yilmaz, 2001); the main one is the fact that it has an improved signal-to-noise ratio (SNR) when compared to the pre-stack traces.

In order to stack seismic signals we must perform previous operations in the seismic traces. The operations with more influence in the stacking are the normal moveout (NMO) correction and velocity analysis. The NMO correction is an operation which aims to correct the time delays (also known as moveouts) in consecutive traces, in order to add the traces constructively in the stacking operation (Yilmaz, 2001). The velocity analysis consists in the estimation of the velocities for the NMO correction (Yilmaz, 2001).

Several characteristics of seismic wave propagation may affect the stacking of seismic data. In this paper we address the issues caused by reflections that occur at angles larger than the critical angle, which are known as *post-critical* or *super-critical* reflections. These reflections differ from the normal ones because they cause changes in the phase of seismic signals. These phase changes significantly impact the stacking operation. In order to constructively stack the seismic traces, it is common practice in seismic processing discard all the traces with post-critical reflections. This situation can significantly diminish the number of traces used for stacking, for instance, when dealing with shallow water reflections in the marine case.

In order to deal with the phase change in post-critical reflections of seismic signals, in this paper, we propose a methodology which makes use of the complex seismic analytic signal, obtained with the use of the Hilbert transform (Taner et al., 1979), and the singular value decomposition (SVD) (Peterson and DeGroat, 1988). We named this methodology of *phase equalization* and it must be performed together with the NMO correction. In the next sections we explain NMO correction and stacking in detail. Then, we explain the proposed phase equalization methodology. We also show two numerical experiments that we performed with synthetic data. The initial results indicate that the phase changes can be corrected using the complex signals. These results must be further confirmed by simulations on real data.

Normal moveout

In order to understand the normal moveout (NMO) correction, we first describe the seismic acquisition geometry. In Fig. 1(a) we show the recording geometry, which is also known as common-shot geometry, and the ray paths associated with a horizontal reflector. Fig. 1(a) illustrates a typical 2D acquisition, with source and receivers placed in a single line (Yilmaz, 2001). We also assume, in this paper, 2D geometries. We define s and g_i as the positions of source and receivers in the acquisition line. The index i varies from 1 to the maximum number of receivers at each shot. The seismic trace corresponds to the time samples recorded at a given receiver with position g_i, associated to a shot fired at the position s. The source-receiver coordinates of that trace are given by the pair (s, g_i).

In Fig. 1(b) we show the common-midpoint (CMP) geometry, with the ray paths associated with a horizontal reflector as well. The CMP gather is formed by grouping traces with the same midpoint, even if they come from different shots. For the CMP geometry we define y and h_j, which are, respectively, the midpoint and half-offset coordinates. These coordinates are given by $y = (g_j + s_j)/2$ and $h_j = (g_j - s_j)/2$. Note that h_j is half the distance between source and receiver and j varies from 1 to the maximum number of receivers at each CMP gather.

The CMP geometry allows us to combine the reflections from different traces of the CMP gather. This is possible because, as shown in Fig. 1(b) for the horizontal reflector situation, the reflections come from the same point in depth. The combination of seismic traces from the same CMP gather may also increase the signal-to-noise (SNR) ratio, since the reflections in the traces were recorded at

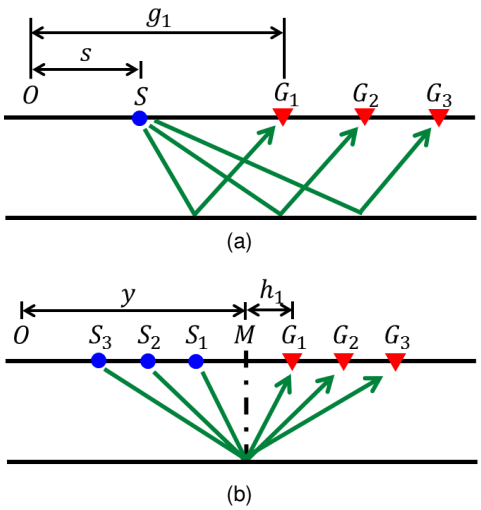

Figure 1: (a) Common shot and (b) common-midpoint geometries.

different locations and time instants and were probably corrupted by independent noise samples.

To properly combine the reflections in the CMP gather, we need to estimate and correct the delays of the reflections in each trace. These delays are known as moveouts. The moveouts estimation is done by considering the traveltime of a zero-offset trace, for which both source and receiver are *virtually* placed at y. For a known velocity, this traveltime is related to that of the other traces. In the CMP gather configuration, a well accepted traveltime is the normal moveout (NMO) (Yilmaz, 2001), given by

$$t^2(t_0,h) = t_0^2 + \frac{4h^2}{v^2}, \tag{1}$$

where t_0 denotes the two-way zero-offset traveltime and v can be viewed as an effective velocity.

The velocity in (1) must be estimated and the most widely used technique is the velocity analysis (Neidell and Taner, 1971). In the next section we discuss this process in more detail.

Velocity analysis

The procedure of velocity analysis is largely employed in seismic signal processing. It consists in, for each t_0, to design, with different velocities v, several traveltime curves using equation (1). The velocity used in the NMO operation is the one that results in a maximum value of a coherence function. The most employed coherence function in seismic processing is the *semblance* (Taner and Koehler, 1969). In the seismic literature, we can find coherence functions based in eigenstructure methods that lead to velocity spectra with higher resolution than semblance (Biondi and Kostov, 1989; Kirlin, 1992). These eigenstructure methods make use of the the Multiple Signal Classification (MUSIC), introduced in (Bienvenu and Kopp, 1980; Schmidt, 1981, 1986), which is based in some properties of the eigendecomposition of the data.

All these coherence measures aforementioned are based in a structure known as the seismic windowed data matrix (Biondi and Kostov, 1989; Kirlin, 1992). The windowing operation consists in, for a given velocity v and t_0, construct a matrix with $L = (N_t - 1)/2$ time samples above and below the sample given by equation (1), at each trace of a CMP gather. The dimension of the windowed data matrix $\mathbf{D}$ is $N_r \times N_t$, with N_r being the number of traces in the CMP and N_t being the number of time samples in the window. When a window with correct values of t_0 and v is applied, the windowed data matrix contains several repetitions of the reflection, all arriving at the same time instant at all the receivers, plus noise terms. In this case, $\mathbf{D}$ can be written as

$$\mathbf{D} = \mathbf{1}\mathbf{s}^T + \mathbf{N}, \tag{2}$$

where $\mathbf{s}$ is an $N_t \times 1$ vector that contains the samples from the reflected wavelet, $\mathbf{1}$ is a $N_r \times 1$ vector of ones, $\mathbf{N}$ is an $N_r \times N_t$ noise matrix independent of $\mathbf{s}$, which may also contain interfering reflections, and the superscript T refers to the transpose operation.

As shown in (Biondi and Kostov, 1989; Kirlin, 1992), the semblance coherence function may be written in terms of the seismic windowed data matrix $\mathbf{D}$ as

$$S = \frac{\mathbf{1}^T \hat{\mathbf{R}} \mathbf{1}}{N_r \mathrm{Tr}\{\hat{\mathbf{R}}\}}, \tag{3}$$

where $\hat{\mathbf{R}} = (\mathbf{D}\mathbf{D}^T/N_t)$ is the spatial covariance matrix of $\mathbf{D}$, $\mathbf{1}$ is a column vector of ones and $\mathrm{Tr}\{\cdot\}$ denotes the trace operator. The value of S falls within the interval $[0,1]$.

The semblance is computed for several values of t_0 and v, resulting into the so-called *velocity spectrum*. For each t_0, the NMO velocity is picked from the velocity spectrum as the one which resulted in the largest semblance.

Stacking

Stacking is the operation which *virtually* generates the ZO trace, once it cannot be generated in practice since, in this case, firing the source would damage the receiver. To generate the stacked ZO trace, and understand how it improves the SNR, notice that, as described in (Barros et al., 2014), when we have a window with good parameters, than the rows of the data matrix $\mathbf{D}$ correspond, approximately, to copies of the same reflection event, but subject to different noise samples. Also note that the center of this window is aligned with the ZO traveltime t_0. Thus, we can generate the sample of the ZO trace at t_0 by taking the average of the samples in the center of the window. Mathematically, this is equivalent to saying that the ZO trace at t_0 is given by the value in the middle coordinate of the estimated wavelet in:

$$\hat{\mathbf{s}} = \frac{1}{N_r}\mathbf{D}^T\mathbf{1}. \tag{4}$$

The operation in equation (4) computes the average of the columns of $\mathbf{D}^T$. Using again the approximation in (2), we see that this average should give us an estimate of the seismic wavelet $\mathbf{s}$. Now, recall that, if t_0 and v are correct, then all the traces in the window contain repetitions of $\mathbf{s}$.

As with the velocity analysis, for stacking seismic data we should repeat the following procedure for each t_0: given t_0, we have a velocity v chosen in the velocity analysis; each pair t_0 and the corresponding v generates a data matrix $\mathbf{D}$;

for each $\mathbf{D}$ we compute $\hat{\mathbf{s}}$ according to (4); and we assign the center entry of $\hat{\mathbf{s}}$ to the sample of the ZO trace at t_0. The value of t_0 is increased according to the desired sampling rate, and the process is repeated.

In many ways, stacking is related to semblance. In fact, it is not hard to show that the semblance can be computed as

$$S = \frac{N_r}{N_t^2} \frac{\|\hat{\mathbf{s}}\|^2}{\mathrm{Tr}\{\mathbf{D}\mathbf{D}^T\}}. \quad (5)$$

Thus, we can think of the semblance as a measure that compares the energy of the stacked data, $\|\hat{\mathbf{s}}\|^2$, with the total energy in the data window, $\mathrm{Tr}\{\mathbf{D}\mathbf{D}^T\}$. The parameters t_0 and v are chosen so as to give a large energy for the stacked signal $\hat{\mathbf{s}}$.

On the other hand, we have seen that the use of MUSIC yields a velocity spectrum with much better resolution than semblance (Biondi and Kostov, 1989; Kirlin, 1992; Barros et al., 2014). Given the parallel between semblance and stacking, a natural question is, then, if we can devise a stacking method that inherits the higher resolution of MUSIC. One approach in this direction is to adapt MUSIC. In its current form, MUSIC provides a sort of spectrum, a measure of the presence of energy in a given window. We intend to adapt this method, so that it provides an estimate of the amplitude of the signal in the window. Similar results following these lines were shown in (Couillet and Kammoun, 2014).

Phase equalization

Let us now reinterpret the approximation for the data matrix in (2). We begin by considering the possibility of using complex traces, obtained as the Hilbert transform of the seismic data (Taner et al., 1979). Thus, we assume complex traces, so that the actual wavelet is given by the real part of the complex wavelet, $\Re\{\mathbf{s}\}$. To allow for the use of complex signals, we henceforth adopt the use of the Hermitian instead of the transpose. Furthermore, we note that, in (2), we assume that the wavelet appears with the same amplitude in all the sensors. Obviously, this is not a good approximation, and we should perhaps write

$$\mathbf{D} = \mathbf{h}\mathbf{s}^H + \mathbf{N}, \quad (6)$$

where $\mathbf{h} = [h_1, h_2, \ldots, h_{N_r}]$ is a vector with the amplitude and the phase of the wavelet in each receiver. Note that the use of $\mathbf{s}^H$ indicates that we are actually modeling the data matrix in terms of the conjugate of the wavelet, not the wavelet itself. However, in the end, we are interested in the real part of the complex wavelet, so that the use of $\mathbf{s}$ or its conjugate is immaterial. Since this makes the notation clearer, we will continue to use the conjugate of $\mathbf{s}$.

Under the model in (6), the best estimate for the wavelet, in the sense of maximizing the SNR, is given by the matched filter (Kay, 1993):

$$\hat{\mathbf{s}} = \frac{1}{\|\mathbf{h}\|^2}\mathbf{D}^H\mathbf{h}. \quad (7)$$

This expression allows for an interesting, albeit obvious, interpretation. Stacking, as defined above, computes the average of the data matrix. This is equivalent to using $\mathbf{h} = \mathbf{1}$ in the matched filter in (7), as was already done in (4). In other words, the traditional stacking operation is optimal when the wavelet appears with the same amplitude and phase in all receivers. Note that (7) has been known in the geophysical literature for a long time, at least for the real case (Robinson, 1970; Mayne, 1962).

In general $\mathbf{h}$ is unknown. Thus, instead of using the actual matched filter, in general it is usual to estimate the wavelet as

$$\hat{\mathbf{s}} = \mathbf{D}^H\mathbf{w}. \quad (8)$$

The search for a vector $\mathbf{w}$ that approximates the matched filter, thus improving stacking, has a rich history in the literature (Grion and Mazzotti, 1998; Peterson and DeGroat, 1988; Liu et al., 2009). Here, we propose to estimate $\mathbf{h}$ using the singular value decomposition (SVD) of the data matrix $\mathbf{D}$. A similar approach was followed in (Grion and Mazzotti, 1998). Our approach is, in many ways, more general, among other reasons for the use of the complex trace.

To see how the SVD can be used to estimate $\mathbf{w}$, consider the SVD of the approximation in (6). Let σ be its largest singular value, and let $\mathbf{u}$ and $\mathbf{v}$ be the corresponding left and right eigenvectors. Thus, we may write

$$\mathbf{D} = \sigma\mathbf{u}\mathbf{v}^H + \mathbf{W}. \quad (9)$$

The matrix $\sigma\mathbf{u}\mathbf{v}^H$ is known as the first eigenimage of $\mathbf{D}$, and can be shown to be the best rank-one approximation to $\mathbf{D}$ (Horn and Johnson, 2012). Note that the signal component of $\mathbf{D}$ in (6) also has rank one. Thus, we may write

$$\sigma\mathbf{u}\mathbf{v}^H \approx \mathbf{h}\mathbf{s}^H. \quad (10)$$

In the literature, the matrix $\sigma\mathbf{u}\mathbf{v}^H$ is said to form the signal subspace of the data (Scharf and Friedlander, 1994). Furthermore, note that, ideally, the matrix $\mathbf{W}$ contains only noise. Thus, ignoring this matrix should improve the SNR of the signal.

Now, using (10), we see that the left and right eigenvectors are proportional to $\mathbf{h}$ and $\mathbf{s}$, so that we may write

$$\mathbf{h} \approx \alpha\mathbf{u} \quad (11)$$

$$\mathbf{s} \approx \beta\mathbf{v}. \quad (12)$$

A few observations are in order. It is interesting to observe that when the SVD is computed, its output has $\|\mathbf{u}\|^2 = \|\mathbf{v}\|^2 = 1$. This implies that $|\alpha| = \|\mathbf{h}\|$ and $|\beta| = \|\mathbf{s}\|$. Also note that these constraints say nothing about the phase of α and β. However, using again (11) and (12) in (10), we may see that the following relation holds:

$$\alpha\beta^* \approx \sigma. \quad (13)$$

This equation is the only constraint we have on the values of α and β, so the SVD does not provide enough information for us to determine $\mathbf{h}$, which requires knowledge of α and $\mathbf{u}$. In fact, this problem has a phase ambiguity: for any pair α and β satisfying (13), and any phase θ, then $\alpha e^{j\theta}$ and $\beta e^{-j\theta}$ also satisfy (13).

To solve the phase ambiguity θ, and to solve the underdetermined equation in (13), we propose to study several assumptions on $\mathbf{h}$. This approach is already followed in the literature where, as mentioned before, the widely used stacking operation is equivalent to the assumption that $\mathbf{h} = \mathbf{1}$. We propose several other approaches, including:

1. We assume that the first entry of $\mathbf{h}$, h_1, is equal to one. This is equivalent to assume that $\alpha = 1/u_1$ and, thus, from (11) we have:

$$\hat{\mathbf{h}} = \frac{\mathbf{u}}{|u_1|}. \tag{14}$$

Where $\hat{\mathbf{h}}$ is the estimate of $\mathbf{h}$. Thus, we may stack the data using (8), where the approximated matched filter is given by

$$\mathbf{w} = u_1^* \mathbf{u}. \tag{15}$$

2. We assume that all entries of $\mathbf{h}$ have unit magnitude, and their phase is given by the phase of $\mathbf{u}$. In this case, we need to solve for the phase ambiguity θ. To that end, we may assume that the phase of h_1 is zero, which is equivalent to saying that $\theta = -\arg\{u_1\}$. In this case,

$$\hat{\mathbf{h}} = [\mathrm{e}^{-j(\arg\{u_1\}+\theta)}\ \mathrm{e}^{-j(\arg\{u_2\}+\theta)} \ldots \mathrm{e}^{-j(\arg\{u_{N_r}\}+\theta)}]. \tag{16}$$

and

$$\mathbf{w} = \frac{\hat{\mathbf{h}}}{N_r}. \tag{17}$$

Thus, in this approach we neglect the difference between the magnitudes of the elements of $\mathbf{h}$ and its relationship to $\mathbf{u}$ as modeled in (11) and we focus on the correction of the phase. Also, it is interesting to notice that if all entries of $\hat{\mathbf{h}}$ are real, i.e., equal to one, then using (17) in (8) results in regular stacking, i.e., the stacked trace becomes the average of the traces in the window.

3. We may use the later approach, but instead of estimate the phase by $\theta = -\arg\{u_1\}$ we estimate it by the average of all the phases from $\mathbf{u}$:

$$\theta = -\frac{1}{N_r}\sum_{i=1}^{N_r} \arg\{u_i\}. \tag{18}$$

Previous results

One post-critical reflection

In this numerical example we used a synthetic CMP with one single reflection, generated by ray-tracing. To generate the data we considered one homogeneous layer with the depth of 250 m and interval velocity of 1500 m/s. This layer presents an interface with another layer with interval velocity of 1800 m/s. The data is shown in Fig. 2. It is possible to observe the change in the wavelet shape after the critical angle, which is located in the offset of 753 m. The blue lines in Fig. 2 indicate a window with samples around the center of the wavelet, designed with the velocity of the center of the wavelet, picked from a semblance coherence panel. In Fig. 3(a) we show the result of performing the windowing operation to select the reflection. It is possible to observe the change in the phase with the increase of the offset. In Fig. 3(b) we apply the the windowing operation with phase equalization using the second approach from previous section. We observe that the phase shift was complectly corrected.

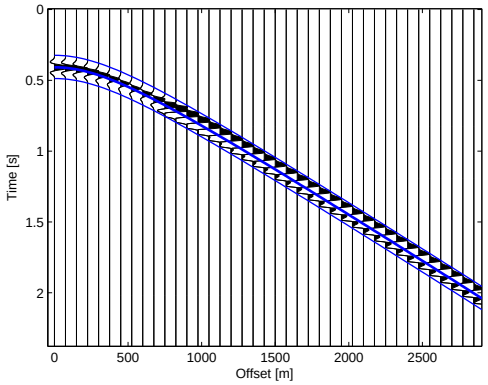

Figure 2: Synthetic data with one post-critical reflection, after the offset of 753 m. The blue lines indicate a window with samples around the center of the wavelet, designed with the velocity of the center of the wavelet, picked from a semblance coherence panel.

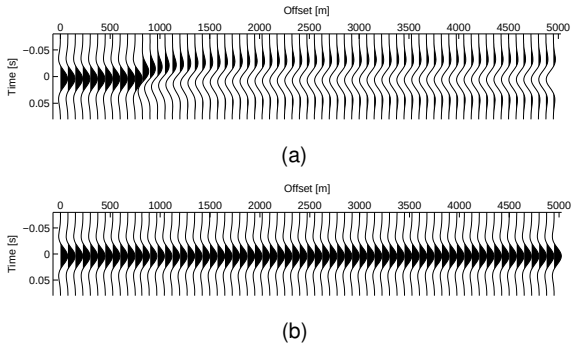

Figure 3: (a) Regular NMO operation in the window of Fig. 2. (b) Phase equalization and NMO operation in the window of Fig. 2.

CMP with several post-critical reflections

We present now a numerical example with a more complex synthetic data. We generated this data also with ray-tracing, based in a model with six homogeneous layers. The reflections of the first three layers present a phase rotation, due to critical angles. We show in Table 1 the model parameters used to generate this data. In Fig. 4 we show the CMP data we generated for this example.

In Fig. 5 we show the NMO corrected CMP family for the data of Fig. 4. The blue dots in Fig. 5 mark the offset after which we only have critical reflections for a given event. Figures 5(a) and 5(b) apply the SVD to filter out non horizontal events; real and complex traces are used in figures 5(a) and 5(b), respectively. For the phase equalization in Fig. 5(b) we adopted the second approach from previous section. In other words, both figures show, for each t_0, the center of the first eigenimage of the data matrix $\mathbf{D}$ using the window with the corresponding t_0 and v. As seen by the top arrows in this figure, the complex trace allows us to deal with post-critical reflections. These reflections differ from the normal ones only in the phase of their Hilbert transforms. As these initial results indicate, this phase change can be corrected using the complex

Table 1: Model parameters for data generation.

	Depth [m]	Velocity [m/s]	t_0 [s]	Critical angle offset [m]
Layer 1	250	1500	0.33	753.78
Layer 2	650	1800	0.78	3010.5
Layer 3	1250	1900	1.41	1056.9
Layer 4	1450	4600	1.50	No critical angle
Layer 5	1950	2100	1.97	No critical angle
Layer 6	2500	2200	2.47	No critical angle
		2300		

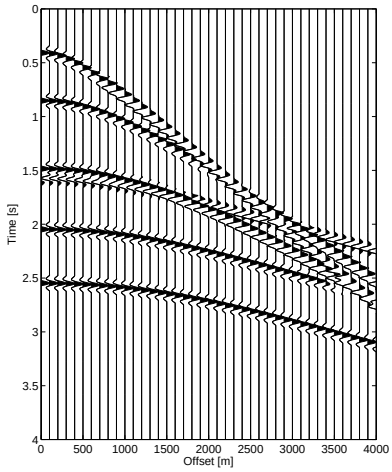

Figure 4: Synthetic CMP with several post-critical angle reflections.

signals. If this result proves to be robust, we may correct for the phase change and coherently combine post- and pre-critical reflections. In the literature, these two types of reflections are normally treated separately. It is possible to observe in Fig. 5 artifacts between the reflections. These artifacts are caused because coherent events appear in the velocity analysis and NMO correction for t_0 where there are no events. We are currently investigating these appearance of artifacts and methods for its mitigation.

The main motivation for studying the complex trace was the phase equalization of post-critical reflections. However, Fig. 5 suggests that the complex trace may have other benefits. In fact, as indicated by the bottom arrows in both figures, the complex traces seem to be able to correct small delays between traces, making the processing more robust to events that are not perfectly aligned. In this particular case, the misalignment is caused by a mismatch between the NMO traveltime in (1) and the actual traveltime. However, the misalignment is also common in land data, where residual static corrections must be applied to the data (Marsden, 1993). Also, as indicated by the middle arrows, the complex trace seems to do a better job at cancelling interfering events. Obviously, these results must be further confirmed by simulations on real data and by a careful analysis of the expected performance of the method, and an explanation for all these apparent benefits.

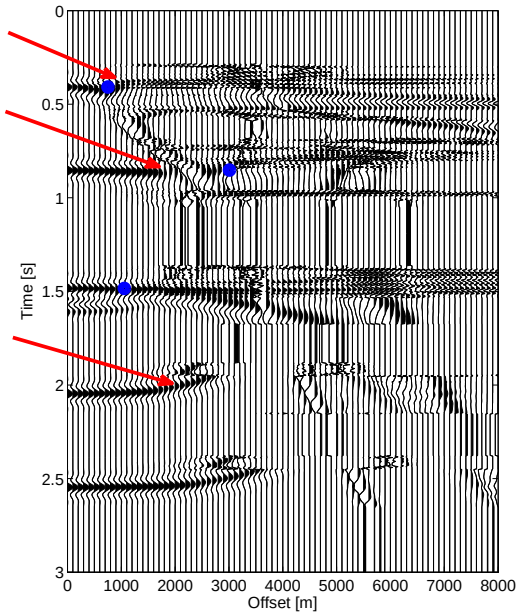

(a)

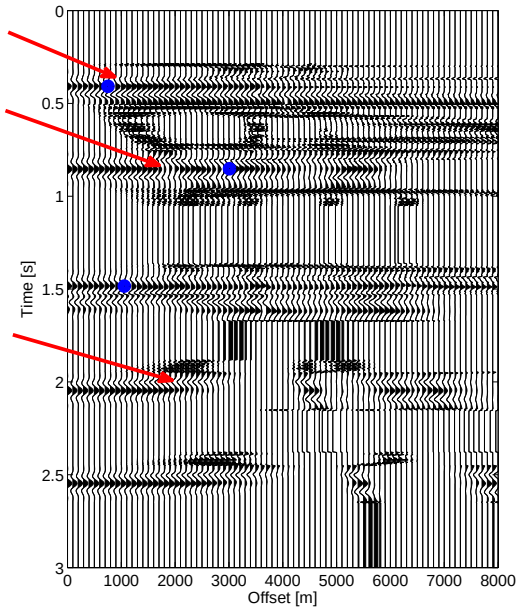

(b)

Figure 5: CMP gather after NMO correction. To filter out non-horizontal events, for each t_0 we use only the first eigenimage of the data window of the real (in figure a) or the complex (in figure b) trace. The top arrows indicate the point where the complex trace is able to compensate for the phase change of the post-critical reflection. The middle arrow indicates a point where the complex trace improves the elimination of an interfering event. The bottom arrow shows a point where the complex trace corrects for timing errors. The blue dots in these figures mark the offset after which we only have critical reflections for a given event.

Conclusions

In this paper we addressed the phase equalization of seismic signals for the normal moveout correction and stacking operations. Seismic signals may present large deviations in phase, especially in the case of post-critical reflections. This can lead to situations where only few traces are used for the stacking operation. We proposed a method for phase equalization which employs the first eigenimage obtained with the use of the singular value decomposition of the analytical signal of seismic windowed data. We also suggested different methods for the phase estimation, which employ the SVD. We tested our proposal in two synthetic data, both of them with post-critical reflections. The first synthetic data presented only a single reflection, but the second data was more complex, with more reflections. The first example indicates that the phase shift caused by reflections after the offset of post-critical angles can be correct by the use of the phase equalization method. The initial results of the second example also indicate that the phase change can be corrected using the complex signals. If the proposed method proves to be robust, we may correct for the phase change and coherently combine post- and pre-critical reflections. The second example also indicates that the complex trace seems to do a better job at cancelling interfering events. Obviously, these results must be further confirmed by simulations on real data and by a careful analysis of the expected performance of the method.

Acknowdegments

The authors thank CNPq, INCT-GP/CNPQ (www.inct-gp.org) and PETROBRAS for the financial support.

References

Barros, T., R. Lopes, and M. Tygel, 2014, Implementation aspects of eigendecomposition-based high-resolution velocity spectra: Geophysical Prospecting, **63**, 99–115.

Bienvenu, G., and L. Kopp, 1980, Adaptivity to background noise spatial coherence for high resolution passive methods: Acoustics, Speech, and Signal Processing, IEEE International Conference on ICASSP '80., 307–310.

Biondi, B. L., and C. Kostov, 1989, High-resolution velocity spectra using eigenstructure methods: Geophysics, **54**, 832–842.

Couillet, R., and A. Kammoun, 2014, Robust g-music: Presented at the 22nd European Signal Processing Conference (EUSIPCO).

Grion, S., and A. Mazzotti, 1998, Stacking weights determination by means of svd and cross-correlation: 68th Annual International Meeting, Society of Exploration Geophysicists, Expanded Abstract, 1135–1138.

Horn, R. A., and C. R. Johnson, 2012, Matrix analysis: Cambridge university press.

Kay, S. M., 1993, Fundamentals of statistical signal processing, volume i: Estimation theory: Prentice Hall Signal Processing Series.

Kirlin, R. L., 1992, The relationship between semblance and eigenstructure velocity estimators: Geophysics, **57**, 1027–1033.

Liu, G., S. Fomel, L. Jin, and X. Chen, 2009, Stacking seismic data using local correlation: GEOPHYSICS, **74**, V43–V48.

Marsden, D., 1993, Static corrections-a review, part iii: The leading edge, **12**, 210–216.

Mayne, W. H., 1962, Common reflection point horizontal data stacking techniques: Geophysics, **27**, 927–938.

Neidell, N., and M. Taner, 1971, Semblance and other coherency measures for multichannel data: Geophysics, **36**, 482–497.

Peterson, J. B., and R. D. DeGroat, 1988, Nearly optimal, svd-based stacking of seismic data: Signals, Systems and Computers, 1988. Twenty-Second Asilomar Conference on, IEEE, 858–862.

Robinson, J. C., 1970, Statistically optimal stacking of seismic data: Geophysics, **35**, 436–446.

Scharf, L., and B. Friedlander, 1994, Matched subspace detectors: Signal Processing, IEEE Transactions on, **42**, 2146–2157.

Schmidt, R., 1981, A signal subspace approach to multiple emitter location and spectral estimation.

——, 1986, Multiple emitter location and signal parameter estimation: Antennas and Propagation, IEEE Transactions on, **34**, 276–280.

Taner, M. T., and F. Koehler, 1969, Velocity spectra—digital computer derivation applications of velocity functions: Geophysics, **34**, 859–881.

Taner, M. T., F. Koehler, and R. Sheriff, 1979, Complex seismic trace analysis: Geophysics, **44**, 1041–1063.

Yilmaz, O., 2001, Seismic data analysis: Processing, inversion, and interpretation of seismic data, volume 1, 2nd ed.: Society of Exploration Geophysicists. Investigations in Geophysics.